Ultimate Axial Load Capacity of a Delaminated Beam-Plate

Wan-Lee Yin,* Sayed N. Sallam,† and George J. Simitses‡
Georgia Institute of Technology, Atlanta, Georgia

The paper presents elastic buckling and postbuckling analysis of an axially loaded beam-plate with an across-the-width delamination symmetrically located at an arbitrary depth. It is found that, for a relatively short and thick delamination, the buckling load of the delaminated plate is a close lower bound of the ultimate axial load capacity. In the case of a relatively slender delamination, the postbuckling axial load can be considerably greater than the buckling load, while the failure of the plate may or may not be governed by delamination growth. The energy-release rate associated with delamination growth is systematically computed for various combinations of the delamination length and axial load. The resulting curves determine the possibility and the stability characteristics of delamination growth and provide a basis for finding the ultimate axial load capacity.

Nomenclature

a = half-length of delamination
h = thickness of delamination
ℓ = half-length of the plate
t = thickness of the plate
$\bar{a}$ = a/ℓ
$\bar{h}$ = h/t
α = $\bar{a}/\bar{h}$
P_i = axial forces
M_i = bending moments
u, v, w = transverse deflections
D_i = bending stiffnesses
κ, λ, μ = (P_i/D_i), $i = 1,2,3$
E = Young's modulus in the axial direction
A = amplitude of deflection
θ = $(A\kappa \sin \kappa b)/2$
$(P_1)_{cr}$ = critical value of P_1
P_1^* = ultimate value of P_1
G = energy release rate
$\bar{G}$ = $G\ell^4/(Et^5)$
$\bar{P}$ = $(\kappa\ell/\pi)^2$
G^* = critical value of G
$\bar{G}^*$ = $G^*\ell^4/(Et^5)$

I. Introduction

DELAMINATION of a composite laminate reduces the overall stiffness and thereby lowers the buckling load of the laminate. The latter may or may not be a useful indication of the load-carrying capacity of the delaminated plate. In some cases, it may be significantly smaller than the elastic collapse load in the postbuckling regime, especially if the laminate contains a relatively long and thin delamination. In order to determine the ultimate load capacity, it is necessary to obtain the elastic postbuckling solution of the delaminated plate and, furthermore, to examine the possibility and the process of delamination growth by considering the fracture toughness of the material.

The case of a one-dimensional delamination (i.e., an across-the-width delamination in an axially loaded rectangular plate), although perhaps an oversimplified mathematical model, is amenable to an exact analysis on the basis of the Euler-Bernoulli theory of beam-plates.[1,2] While Chai et al.[1] computed the energy-release rate associated with delamination growth by numerical differentiation of the total potential energy with respect to delamination length, Yin and Wang[2] obtained, by means of the path-independent J integral, an algebraic expression of the energy-release rate in terms of the axial forces and bending moments acting across the various cross sections adjacent to the tip of delamination. This allows straightforward evaluation of the energy-release rate whenever a postbuckling solution is known. The initiation and the subsequent process of delamination growth can be analyzed on the basis of a Griffith-type fracture criterion.

In the present analysis, we consider a specially orthotropic rectangular plate axially loaded along two clamped edges. It is assumed that, at an arbitrary distance from the top or bottom surface of the plate, an across-the-width delamination is located symmetrically with respect to the two clamped edges and remains so in the course of delamination growth. For each given length of delamination, the plane strain postbuckling solution depends on the applied axial load as does the energy-release rate. General expression of the postbuckling solution, as well as the algebraic equations governing the amplitude of deflection, are presented in Sec. II. In Sec. III we obtain a special type of postbuckling solution that is not included in the general expression and that occurs only if an appropriate axial load is applied to a plate containing a sufficiently long delamination. This special postbuckling solution marks the transition of postbuckling deformation from an initial phase, experienced by all delaminated plates, to a second phase that is peculiar to plates with relatively long delaminations.

The analysis in Secs. IV and V indicates that there are two distinctive types of postbuckling processes and that the occurrence of each type depends on the relative slenderness of the delamination vs the plate. In the case of a short and thick delamination, the axial load in the plate never deviates significantly from the critical buckling load. The postbuckling solution changes from states in which the crack is completely open to a state in which it is fully closed. Henceforth, postbuckling deformation continues at *constant* axial load provided that the crack does not extend and that there is smooth contact along

Presented as Paper 84-0892 at the AIAA/ASME/ASCE/AHS 25th Structures, Structural Mechanics and Materials Conference, Palm Springs, CA, May 14-16, 1984; received Aug. 3, 1984; revision received March 11, 1985.

*Professor. Member AIAA.
†Graduate Research Assistant.
‡Professor. Associate Fellow AIAA.

the crack (Sec. IV). On the other hand, buckling of a plate containing a thin, long delamination is initiated by local buckling of the delaminated layer. In the postbuckling regime, the axial load may become significantly larger than the critical buckling load, so that the latter is not a close estimate of the load capacity. *Partial* contact of the crack starts at the crack tip when the axial load has passed its peak value and is slowly decreasing (Sec. V). Although the axial load capacity of the plate is bounded above by the peak value, it is not necessarily equal to the latter because the crack growth may occur before the axial load reaches its peak value. The relation between the normalized axial load $\bar{P}$ and the normalized energy-release rate $\bar{G}$ under a fixed delamination length can be represented by a curve in the $\bar{G}$-$\bar{P}$ plane. A one-parameter family of such curves is generated as the delamination length varies. The use of these curves for the evaluation of the ultimate load capacity of delaminated plates is discussed in Sec. VI with the assumption of a Griffith-type fracture criterion.

The present work presents an analytical procedure for evaluating the ultimate load capacity of a laminate containing a one-dimensional delamination. Postbuckling solutions and energy-release rates are computed for three cases corresponding, respectively, to a relatively thick, a relatively thin, and an extremely thin delamination. The dependence of the energy-release rate upon the delamination length and the axial load is similar in kind, although different in degree, in all three cases. This suggests that a common computational scheme may be used to obtain the ultimate load capacities, irrespective of the thickness of delamination.

II. Buckling and Postbuckling Behavior

We consider a homogeneous, orthotropic beam-plate of thickness t containing a parallel plane crack at a depth h ($h \leqq t/2$) from the top surface of the plate. The plate has a constant width between two lateral edges and it is subjected to compressive axial loads at the clamped ends $x = \pm \ell$. As shown in Fig. 1, the crack extends over an interval $-a \leqq x \leqq a$ and runs across the whole width of the plate. It is convenient to refer to the crack as a "delamination," even though the plate does not possess a laminated structure. The delaminated plate starts to buckle when the axial load reaches a critical value. If appropriate boundary conditions are maintained along the lateral edges, the plate undergoes cylindrical bending deformation in the postbuckling states. By using the symmetry condition with respect to the midpoint, the clamped boundary conditions at the two ends, and the continuity of deflection and slope at the crack tip, one may obtain the following expressions for the upward postbuckling deflection of the intact segment and of the lower and upper detached segments, respectively[3]:

$$u(x) = A[1 - \cos\kappa(\ell - x)], \quad a \leqq x \leqq \ell \tag{1a}$$

$$v(x) = A\left[\frac{\kappa \sin\kappa b}{\lambda \sin\lambda a}(\cos\lambda x - \cos\lambda a) + 1 - \cos\kappa b\right], \quad 0 \leqq x \leqq a \tag{1b}$$

$$w(x) = A\left[\frac{\kappa \sin\kappa b}{\mu \sin\mu a}(\cos\mu x - \cos\mu a) + 1 - \cos\kappa b\right], \quad 0 \leqq x \leqq a \tag{1c}$$

where

$$b = \ell - a, \quad \kappa^2 = P_1/D_1, \quad \lambda^2 = P_2/D_2, \quad \mu^2 = P_3/D_3 \tag{2}$$

and P_i and D_i ($i = 1,2,3$) are the compressive forces and the bending stiffnesses of the various segments which undergo deflections u, v, and w, respectively. The amplitude A is determined by the compressive load P_1 in the manner described below. The expressions of Eqs. (1) are valid provided that the crack remains completely open and that $\mu a < \pi$ and $\lambda a < \pi$.

At the crack tip $x = a$, the axial forces P_1, P_2, and P_3 and the bending moments

$$M_1 = D_1 u''|_{x=a}, \quad M_2 = D_2 v''(a), \quad M_3 = D_3 w''(a) \tag{3}$$

satisfy the equilibrium equations

$$P_2 + P_3 = P_1, \quad M_1 = M_2 + M_3 - P_2 h/2 + P_3(t-h)/2 \tag{4}$$

Following Kachanov,[4] one compares the deformed arc lengths of the upper and lower detached segments to obtain a compatibility relation

$$(1 - \nu_{13}\nu_{31})\frac{P_3 a}{Eh} + \frac{1}{2}\int_0^a (w')^2\,dx = (1 - \nu_{13}\nu_{31})\frac{P_2 a}{E(t-h)} + \frac{1}{2}\int_0^a (v')^2\,dx + \frac{w'(a)t}{2} \tag{5}$$

where E is the Young's modulus in the axial direction and $(1 - \nu_{13}\nu_{31}) = Et^3/D_1$. The system of Eqs. (1-5) may be reduced to

$$\theta^2\left(\frac{1}{\sin^2\mu a} - \frac{1}{\mu a \tan\mu a} - \frac{1}{\sin^2\lambda a} + \frac{1}{\lambda a \tan\lambda a}\right) + \theta\frac{t}{a} + \frac{1 - \nu_{13}\nu_{31}}{E}\left(\frac{P_3}{h} - \frac{P_1 - P_3}{t-h}\right) = 0$$

$$\theta = \frac{tP_3 - hP_1}{4b}\left[\frac{P_1}{\kappa b \tan\kappa b} + \frac{a}{b}\left(\frac{P_1 - P_3}{\lambda a \tan\lambda a} + \frac{P_3}{\mu a \tan\mu a}\right)\right]^{-1} \tag{6}$$

where κ and μ are as defined by Eqs. (2) and $\lambda^2 = (P_1 - P_3)/D_2$. For any given value of P_1 that exceeds the critical buckling load, the system of Eq. (6) furnishes two algebraic equations for the two unknowns P_3 and θ. Solution of this system of equations yields the unknown amplitude A in Eq. (1),

$$A = 2\theta/\kappa \sin\kappa b \tag{7}$$

Then Eqs. (1) and (3) yield the transverse deflections and the bending moments of the postbuckling solution.

Immediately after the buckling of the delaminated plate, the deflection amplitude A is small and the two integrals occurring in Eq. (5) are negligible (of the order A^2) in comparison with the remaining terms. Hence,

$$P_3(t-h) - P_2 h \approx \frac{w'(a)\,Eth(t-h)}{2a(1 - \nu_{13}\nu_{31})}$$

Substituting into the second equation of (4) and making use of Eqs. (1) and (3), we obtain

$$D_1\kappa^2\cos\kappa b + D_2\kappa\lambda\sin\kappa b\,\mathrm{ctn}\lambda a + D_3\kappa\mu\sin\kappa b\,\mathrm{ctn}\mu a + \frac{Eth(t-h)}{4a(1 - \nu_{13}\nu_{31})}\kappa\sin\kappa b \approx 0 \tag{8}$$

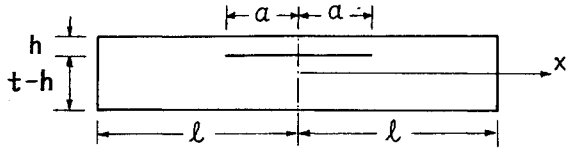

Fig. 1 Geometry of the model.

Let $\bar{h} = h/t$. Then,

$$D_2 = (1-\bar{h})^3 D_1,\ D_3 = \bar{h}^3 D_1 \tag{9}$$

Since $P_2 = (1-\bar{h})P_1$ and $P_3 = \bar{h}P_1$ at the critical state of buckling, Eqs. (2) deliver

$$\lambda_{cr} = \kappa_{cr}/(1-\bar{h}),\quad \mu_{cr} = \kappa_{cr}/\bar{h} \tag{10}$$

Hence, Eq. (8) yields the following characteristic equation for κ_{cr}:

$$\operatorname{ctn}(\kappa_{cr} b) + (1-\bar{h})^2 \operatorname{ctn}\left(\frac{\kappa_{cr} a}{1-\bar{h}}\right) + \bar{h}^2 \operatorname{ctn}\left(\frac{\kappa_{cr} a}{\bar{h}}\right) + \frac{3\bar{h}(1-\bar{h})}{\kappa_{cr} a} = 0 \tag{11}$$

The solution of this characteristic equation determines the buckling load $(P_1)_{cr} = \kappa_{cr}^2 D_1$.

III. A Special Postbuckling Solution

In obtaining the deflection functions of Eq. (1), it was assumed that $\mu a < \pi$ and $\lambda a < \pi$ so that the denominators in Eqs. (1b) and (1c) do not vanish. Since $\bar{h} < 0.5$, Eq. (10) implies that $\lambda_{cr} < \mu_{cr}$. Hence, $\lambda a < \mu a$ in an initial postbuckling stage. For a relatively long delamination, μa attains the value π at an axial load slightly above the buckling load. The postbuckling solution corresponding to the state $\mu a = \pi$ is expressible in the following form:

$$u(x) \equiv v(x) \equiv 0,\quad w(x) = B(1 + \cos \pi x/a)$$

The amplitude B can be determined from the equilibrium equation (4b) and the compatibility equation (5). Since $M_1 = M_2 = 0$ and $v \equiv 0$, these equations reduce to

$$2\bar{h}^3 D_1 \left(\frac{B}{t}\right)\left(\frac{\pi}{a}\right)^2 - P_2\bar{h} + P_3(1-\bar{h}) = 0$$

$$\bar{h}P_2 - (1-\bar{h})P_3 = \frac{Et^3\bar{h}(1-\bar{h})}{4(1-\nu_{13}\nu_{31})}\left(\frac{\pi}{a}\right)^2\left(\frac{B}{t}\right)^2$$

Consequently,

$$B/2 = 2\bar{h}^2/3(1-\bar{h})$$

and

$$P_2 = D_1\left(\frac{\pi\bar{h}}{a}\right)^2\left[1 - \bar{h} + \frac{4\bar{h}^2}{3(1-\bar{h})}\right]$$

Hence, the postbuckling solution and the corresponding axial load are given by

$$u(x) = v(x) = 0,\quad w(x) = t\frac{2\bar{h}^2}{3(1-\bar{h})}\left(1 + \frac{\cos \pi x}{a}\right) \tag{12}$$

$$P_1 = P_2 + \bar{h}^3 D_1\left(\frac{\pi}{a}\right)^2 = D_1\left(\frac{\pi\bar{h}}{a}\right)^2\left[1 + \frac{4\bar{h}^2}{3(1-\bar{h})}\right] \tag{13}$$

Since P_1 must be smaller than the critical buckling load of a perfect plate, $P_1 < \pi^2 D_1/\ell^2$, Eq. (13) yields the following *necessary* condition of the existence of a solution as expressed by Eq. (12):

$$\bar{a} \equiv \frac{a}{\ell} > \bar{h}\left[1 + \frac{4\bar{h}^2}{3(1-\bar{h})}\right]^{\frac{1}{2}} \tag{14}$$

As the axial load increases and surpasses the value given in Eq. (13), the postbuckling solution changes from the general form of Eq. (1) to the special form of Eq. (12) and returns to the general form. The detailed features of this transition are described in Sec. V.

IV. Short Delamination

The ratios $\bar{h} = h/t$ and $\bar{a} = a/\ell$ introduced in the preceding sections can be regarded as the normalized thickness and length of the delamination. Clearly, the restriction of $\bar{h}$ to a range of 0-0.5 does not impair the generality of the analysis.

We now introduce a geometrical parameter α, defined as the ratio of the normalized delamination length to the normalized thickness,

$$\alpha = \bar{a}/\bar{h} = at/\ell h$$

This dimensionless parameter can be considered as a relative slenderness ratio of the thin delamination (length $2a$, thickness h) vs a perfect plate of length 2ℓ and thickness t. Both the critical buckling load and the postbuckling behavior depend sensitively on the value of the parameter α. For a relatively thin delamination, say $h < 0.2$, there are sharp contrasts in buckling and postbuckling behavior between the cases of *short* and *long* delaminations, defined, respectively, by the *approximate* ranges $\alpha < 1$ and $\alpha > 1$. In the present section, we examine the case of a short delamination.

Since the length of delamination is small, the global stiffness of the delaminated plate is close to that of a perfect plate, i.e.,

$$\kappa_{cr}^2 D_1 \approx 4\pi^2 D_1/(2\ell)^2 \tag{15}$$

or

$$\kappa_{cr}\ell/\pi \approx 1 \tag{16}$$

The accuracy of this approximation is well confirmed[3,5] by the numerical solutions of the characteristic equation (11).

In the postbuckling regime, the value of κ changes within a narrow range from κ_{cr} to some upper bound κ^*, which is less than π/ℓ [because the axial load capacity of a delaminated plate $(\kappa^*)^2 D_1$ is necessarily smaller than the buckling load of a *perfect* plate; the latter is given by the right-hand side of Eq. (15)]. So long as the crack remains completely open, the deflection functions have the form of Eq. (1) and the curvature of the buckled plate at the fixed ends is given by

$$u''|_{x=\pm\ell} = A\kappa^2$$

At the midpoint $x = 0$, the curvatures of the lower and upper segments are, respectively,

$$v''(0) = -A\kappa\lambda\frac{\sin \kappa b}{\sin \lambda a},\quad w''(0) = -A\kappa\mu\frac{\sin \kappa b}{\sin \mu a} \tag{17}$$

and the separation of the two segments is

$$w(0) - v(0) = \frac{A}{2}\kappa a \sin \kappa b\left[\frac{\tan(\mu a/2)}{\mu a/2} - \frac{\tan(\lambda a/2)}{\lambda a/2}\right] \tag{18}$$

Since κ varies in a very small range from κ_{cr} to κ^*, Eq. (10) implies the following approximations:

$$\lambda a \approx \frac{\kappa a}{1-\bar{h}} = \frac{\bar{h}}{1-\bar{h}}\alpha\kappa\ell,\quad \mu a \approx \frac{\kappa a}{\bar{h}} = \alpha\kappa\ell \tag{19}$$

where $\bar{h} < 0.5$ and $\kappa \leqq \kappa^* < \pi/\ell$. For a short delamination ($\alpha < 1$), these approximate relations imply the following con-

Fig. 2 Short delamination.

dition for initial postbuckling states:

$$\lambda a \leqq \mu a < \pi$$

Hence the curvatures $v''(0)$ and $w''(0)$ have the same algebraic sign and it is opposite to the algebraic sign of u'' at $x = \ell$. A positive amplitude A corresponds to a positive separation $w(0) - v(0)$ because $\lambda a \leqq \mu a$ and because $(\tan x)/x$ is a monotonic increasing function of x [see Eq. (18)]. Thus, the buckled plate has a profile as shown in Fig. 2. The plate deflects upward so that the buckling deformation relieves the compressive load in the upper delaminated layer and aggravates the load in the lower layer. Hence, μa increases and λa decreases as postbuckling deformation progresses. Eventually, λa becomes equal to μa and Eq. (1) yields $v(x) \equiv w(x)$. Then the two completely detached segments above and below the crack come into full contact. This contact state may correspond to the limiting load $P_1^* = (\kappa^*)^2 D_1$, but usually it occurs at an instant when the axial load P_1 has already passed the peak value and is diminishing, while postbuckling deformation and axial shortening continue to progress. The latter case, of course, involves a process that is stable only in an experiment with monotonically increasing end shortening, but not with an increasing compressive axial force.

Following the contact state $\lambda a = \mu a$, postbuckling deformation progresses at a constant axial load P_1' equal to or smaller than P_1^*, provided that the contact between the upper and lower layers is perfectly smooth. In this final stage, the behavior of the beam-plate is identical to that of the Euler column with a reduced bending stiffness in its middle section. Since $\lambda = \mu$, one may set $w(x) \equiv v(x)$ in Eqs. (1-4) to obtain

$$\kappa^2 = \left[\bar{h}^3 + (1-\bar{h})^3\right]\mu^2 \tag{20a}$$

$$\kappa a \operatorname{ctn}(\kappa b) + \left[\bar{h}^3 + (1-\bar{h})^3\right]\mu a \operatorname{ctn}\mu a + 3\bar{h}(1-\bar{h}) = 0 \tag{20b}$$

Solving κ and μ from the last two equations, one obtains the axial load corresponding to the contact state, $P_1 = \kappa^2 D_1$.

V. Long Delamination

If the geometrical parameter $\alpha = \bar{a}/\bar{h}$ is greater than unity by a certain margin, then buckling of the delaminated plate is initiated by local buckling of the thin delamination, because the delamination is relatively slender in comparison with the whole plate. Since the thin layer of delamination has elastically supported ends, its buckling load, $(P_3)_{cr} = \mu_{cr}^2 D_3$, is close to but less than that of a fixed-end plate of thickness h and length $2a$,

$$\mu_{cr}^2 D_3 \lessapprox \pi^2 D_3/a^2$$

Use of Eq. (10) delivers

$$\kappa_{cr}\ell = \bar{h}\mu_{cr}\ell \lessapprox \pi\bar{h}/\bar{a} = \pi/\alpha \tag{21}$$

The accuracy of this approximation is also confirmed by the numerical solutions of the characteristic equation.[5] The critical value of P_1 corresponding to Eq. (21) is

$$(P_1)_{cr} = \kappa_{cr}^2 D_1 \lessapprox (\pi/\ell\alpha)^2 D_1 \tag{22}$$

Fig. 3a Long delamination: initial postbuckling phase.

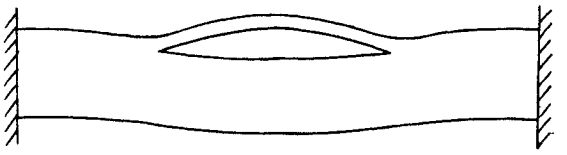

Fig. 3b Long delamination: secondary postbuckling phase.

For $\alpha > 1$, $(P_1)_{cr}$ may be considerably smaller than the buckling load of a perfect plate. Hence, the axial load generally increases far beyond the critical value as postbuckling deformation progresses. A *lower bound* of the ultimate load capacity of the delaminated plate is given by the capacity of a *completely* delaminated plate. The latter is simply the combined axial load capacity of two detached plates. Hence,

$$(\kappa^*)^2 D_1 \geqq \frac{\pi^2 D_2}{\ell^2} + \frac{\pi^2 D_3}{\ell^2} = \left(\frac{\pi}{\ell}\right)^2 D_1\left[\bar{h}^3 + (1-\bar{h})^3\right] \tag{23}$$

As the axial load increases beyond the critical value $\kappa_{cr}^2 D_1$ [Eq. (22)], the approximations of Eqs. (19) and (21) yield, for initial postbuckling states,

$$\kappa\ell \approx \pi/\alpha, \quad \lambda a \approx [\bar{h}/(1-\bar{h})]\pi, \quad \mu a \approx \pi \tag{24}$$

The last estimate shows that the buckled shape of the thin delamination has a wavelength close to the delamination length: $2\pi/\mu \approx 2a$. Hence, $\sin\mu a \approx 0$ and, because $\lambda a \approx \pi\bar{h}/(1-\bar{h}) < \pi$ if $\bar{h}$ is smaller than 0.5 by a certain margin, Eqs. (1) imply that $w(x)$ is considerably greater than $v(x)$. Hence, in the initial postbuckling states, significant transverse deflection occurs mainly in the thin layer of delamination and the deformed profile of the plate has the shape shown in Fig. 3a.

As the axial load increases and postbuckling deformation continues, $\kappa\ell$ deviates increasingly from π/α [Eq. (19a)] and the value of μa very soon surpasses π, as is suggested by Eq. (21). At the transition state $\mu a = \pi$, the postbuckling solution changes its expression from the general form of Eq. (1) to the special form of Eq. (12). The value of $\kappa\ell$ corresponding to this transition state can be obtained from Eq. (13),

$$\kappa\ell = \frac{\pi}{\alpha}\left[1 + \frac{4\bar{h}^2}{3(1-\bar{h})}\right]^{\frac{1}{2}} \tag{25}$$

For a thin delamination ($\bar{h}$ small), the right-hand side of Eq. (25) is only slightly larger than the right-hand side of Eq. (21). Hence, the transition state, which is characterized by the condition $\mu a = \pi$ and Eqs. (25) and (12), occurs at an axial load only slightly larger than the buckling load $(P_1)_{cr}$. As the postbuckling process passes through the transition state, $\sin\mu a$ changes from positive to negative, while λa and κb generally do not change their algebraic signs. Hence, the curvature $v''(0)$, which possesses the same algebraic sign as does $w''(0)$ in the states preceding transition, reverses its algebraic sign after the transition (recall that $v \equiv 0$ and hence $v'' \equiv 0$ in the state of transition). In the transition processes, the main body of the plate changes from upward to downward deflection and the deformed profile of the plate assumes the shape as shown in Fig. 3b. The postbuckling deformation has entered a second

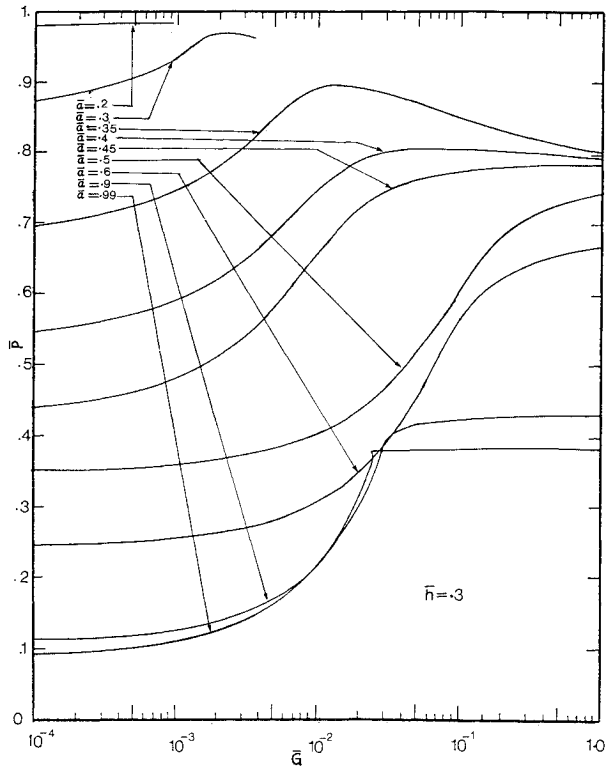

Fig. 4 $\bar{P}$ vs $\bar{G}$ ($\bar{h} = 0.3$).

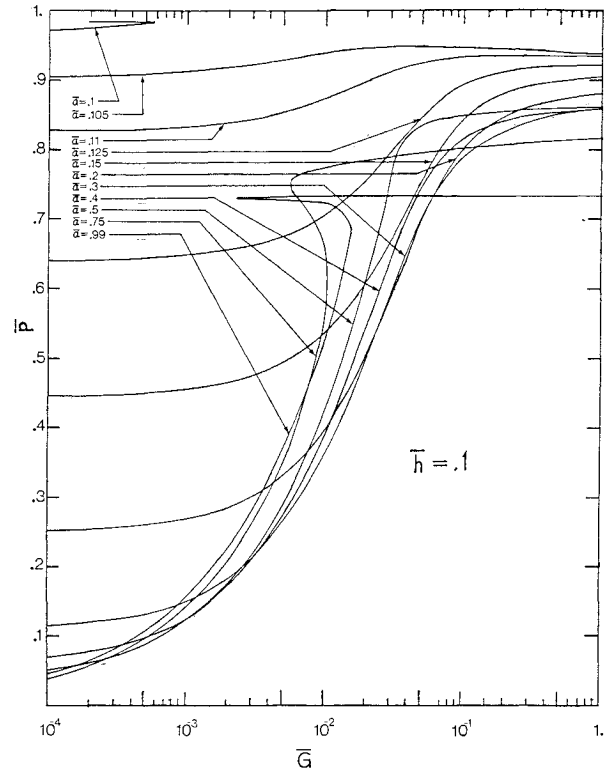

Fig. 5 $\bar{P}$ vs $\bar{G}$ ($\bar{h} = 0.1$).

phase that is characteristic of a relatively long delamination ($\alpha > 1$). Since the wavelength of the buckled delamination, $2\pi/\mu$, decreases with the increase of the axial load, the axial load P_3 in the thin layer of delamination increases with the progress of delamination, instead of being relieved by it. This feature is contrary to the behavior of a relatively short delamination (see Sec. IV).

The condition that the crack remains completely open implies that

$$w''(a) - v''(a) \geqq 0$$

Equation (1) yields

$$w''(a) - v''(a) = \frac{A\kappa \sin \kappa b}{a}\left(\frac{\lambda a}{\tan \lambda a} - \frac{\mu a}{\tan \mu a}\right)$$

In the postbuckling deformation beyond the transition state, $\mu a = \pi$, one has $\pi < \mu a < 3\pi/2$. Eventually, λa exceeds the value $\pi/2$ and at some later stage the factor $(\lambda a/\tan \lambda a - \mu a/\tan \mu a)$ vanishes so that $w''(a) = v''(a)$. Then the crack starts to close at the ends of the delamination. An interior segment of the delamination remains open because $w(0) - v(0)$ as given by Eq. (18) does not vanish with $w''(a) - v''(a)$. Since the crack is *partially* open in the subsequent states, Eq. (1) no longer describes the deflection of the postbuckling solution. Numerical solutions of Eq. (6) indicate that partial closing of the crack generally occurs at a late stage of the postbuckling process when the axial load P_1 has already passed its peak value P_1^* and is slowly diminishing. Hence, the limiting load capacity P_1^* *can* be obtained from the numerical solutions of Eq. (6).

VI. Energy-Release Rate and Ultimate Axial Load Capacity

The preceding analysis of the postbuckling behavior of short and long delaminations assumes that the fracture toughness of the material is sufficiently large to resist the growth of delamination when the plate undergoes the various postbuckling states considered in this analysis. When delamination growth does occur, the geometry of the problem is irreversibly changed. If the fracture behavior of the material is such that delamination growth is governed by a Griffith-type criterion of a critical energy-release rate, then the prediction of whether delamination will grow requires an evaluation of the energy-release rate.

Applying the method of path-independent J integral, Yin and Wang[2] derived a simple algebraic expression for the energy-release rate associated with the growth of a one-dimensional delamination in terms of the axial forces and bending moments acting across the various cross sections adjacent to the delamination front (crack tip),

$$G = \frac{1}{24D_1}\left[\frac{(tP^*)^2}{\bar{h}(1-\bar{h})} + \frac{12(M^*)^2}{\bar{h}^3} + \frac{12(tP^*/2 - M^*)^2}{(1-\bar{h})^3}\right] \tag{26}$$

where

$$P^* = \bar{h}\left[P_1 + 6(1-\bar{h})M_1/t\right] - P_3, \quad M^* = M_3 - M_1\bar{h}^3$$

and P_i and M_i are the forces and moments appearing in Eq. (4). If, for a specified delamination thickness $h = t\bar{h}$ and any given delamination length $2a = 2\ell\bar{a}$, the postbuckling solution corresponding to a given axial load P_1 is computed from Eq. (6), then the energy-release rate associated with the growth of delamination can be directly evaluated from Eq. (26).

Figures 4-6 contain three sets of curves showing the relations between the nondimensionalized energy-release rate, $\bar{G} = \ell^4 G/(Et^5)$, and the normalized axial load, $\bar{P} = (\kappa\ell/\pi)^2$, under fixed geometrical conditions of the delaminated plate. The three figures correspond to the cases $\bar{h} = 0.3$, 0.1, and 0.02. These values of the normalized thickness are thought to be representative of a relatively thick, a relatively thin, and an extremely thin delamination, respectively. Each curve refers to a fixed value of the normalized delamination length $\bar{a}$ and is

obtained from a one-parameter family of numerical solutions of Eq. (6). In the case of relatively long delaminations ($\alpha = \bar{a}/\bar{h} > 1$), $\bar{G}$ varies over a wide range of values as $\bar{P}$ changes. Hence, the curves are plotted in a semilogarithmic diagram. In the case of a short delamination ($\alpha < 1$), postbuckling deformation eventually reaches a state when the two completely detached faces of the crack come into full contact (see Sec. IV). Thus, the associated curve in the $(\bar{G}, \bar{P})$ plane terminates at a $\bar{P}$ value corresponding to the solution of Eq. (20).

In a *quasistatic* process of delamination growth, the energy-release rate $\bar{G}$ maintains a constant critical value $\bar{G}^*$ (the nondimensionalized fracture toughness). As the length of delamination increases, the axial load $\bar{P}$ required to sustain growth changes. The point $(\bar{G}^*, \bar{P})$ moves in a vertical path $\bar{G} = \bar{G}^*$ in the $(\bar{G}, \bar{P})$ plane. Figures 4-6 show that, if the fracture toughness is relatively small, say $\bar{G}^* < 10^{-3}$, then the required axial load $\bar{P}$ *decreases* with delamination growth, although it may slightly increase shortly before the state of complete delamination ($\bar{a} = 1$). Hence, if $\bar{G}^*$ is small, delamination growth under a *constant* axial load $\bar{P}$ (a dead load) is generally a catastrophic process. When a delaminated plate buckles under an increasing axial load P, the postbuckling solution follows one of the curves in the figures until the curve intersects the vertical path $\bar{G} = \bar{G}^*$. The value of $\bar{P}$ at the intersecting point is usually the ultimate axial load capacity of the plate. Afterward, delamination growth starts and proceeds catastrophically if a constant axial load is maintained.

If the length of the existing delamination is relatively short (α small), then $\bar{G}$ never attains the critical value $\bar{G}^*$ and, consequently, delamination growth does not occur. For such plates, the ultimate axial load capacity is not governed by delamination growth, but is determined by its elastic postbuckling behavior. The critical buckling load is a lower bound of, and a close estimate for, the ultimate axial load capacity.

If the fracture toughness is relatively large, say $\bar{G}^* > 0.1$, then in most cases the axial load P also *decreases* with delamination growth in a quasistatic process $\bar{G} = \bar{G}^*$. With certain exceptions, delamination growth under a constant axial load is likewise predominantly unstable and catastrophic. The figures show that in the region of $(\bar{G}, \bar{P})$ plane with $\bar{G} > 0.1$, all curves lie above the horizontal line $\bar{P} = \bar{h}^3 + (1 - \bar{h})^3$. The larger the normalized delamination length $\bar{a}$, the closer is the corresponding $(\bar{G} - \bar{P})$ curve to that horizontal line. If $\bar{h}$ is small and $\bar{G}^* > 0.1$, then the buckling load of a *completely* delaminated plate is a close lower bound of the ultimate axial load capacity.

In the region $10^{-3} < \bar{G} < 0.1$, the curves in the three figures are entangled. For appropriate combinations of $\bar{G}^*$ and initial length $\bar{a}$, delamination growth under a constant axial load *can* be a stable process up to a certain stage of growth. Beyond that stage, however, $\bar{P}$ decreases as $\bar{a}$ increases, implying catastrophic nature of further growth.

It is interesting to note that, for the three figures corresponding to widely different thickness ratios $\bar{h}$, the entanglement of curves is largely restricted to a common region $10^{-3} < \bar{G} < 0.1$. This aside, the dominant feature is that the curves corresponding to larger values of $\bar{a}$ lie *below* the curves corresponding to smaller values of $\bar{a}$. Hence, delamination growth under a constant axial load is, with minor exceptions, generally an unstable process. The axial load at the start of delamination growth (i.e., at the intersection of a curve with the vertical line $\bar{G} = \bar{G}^*$) is always a lower bound of, and in many cases identical with, the ultimate axial load capacity of the delaminated plate.

It should be remarked that although G^* and E are material constants (G^* for carbon-epoxy composites is of the order 1 lb/in.), the nondimensionalized fracture toughness $\bar{G}^* = \ell^4 G^*/(Et^5)$ depends on the length and thickness of the plate. For a given material, $\bar{G}^*$ is large for a slender plate and small for a thick, short plate. Hence, the different regions in the wide scale of $\bar{G}$ can be, and indeed are, relevant to various physical situations. The fracture toughness of many matrix materials may be dependent upon the ratio of the mode I and mode II components of the energy-release rate. This dependence has not been considered in the present analysis because the J integral method does not determine the ratio of model mix.

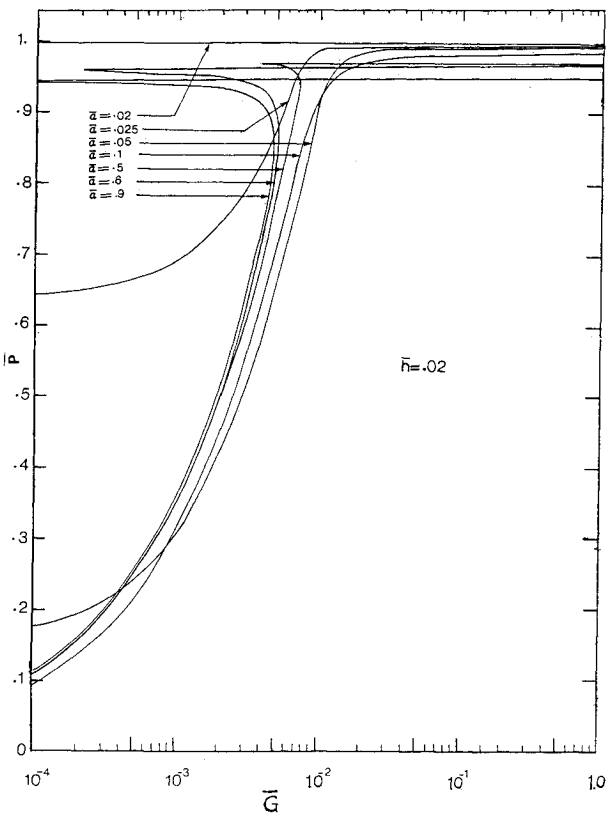

Fig. 6 $\bar{P}$ vs $\bar{G}$ ($\bar{h} = 0.02$).

Corrigendum: The top five curves in Fig. 4 (for $\bar{a} = 0.2$, 0.3, 0.35, 0.4 and 0.45, respectively) were inadvertently misplaced during drawing. They should be shifted one log cycle to the right.

Acknowledgment

This work is supported by the U.S. Air Force Office of Scientific Research through AFOSR Grant-83-0243 to Georgia Institute of Technology. The authors gratefully acknowledge the financial support and express their appreciation to Dr. Anthony K. Amos for his encouragement.

References

[1] Chai, H., Babcock, C.D., and Knauss, W.G., "One Dimensional Modelling of Failure in Laminated Plates by Delamination Buckling," *International Journal of Solids and Structures*, Vol. 17, 1981, pp. 1069-1083.

[2] Yin, W.-L. and Wang, J.T.S., "The Energy-Release Rate in the Growth of a One-Dimensional Delamination," *Journal of Applied Mechanics*, Vol. 51, 1984, pp. 939-941.

[3] Yin, W.-L., Wang, J.T.S., and Fei, Z.-Z., "Damage of Composite Structures, Part II: Stability and Residual Strength of a Delaminated Plate," Georgia Institute of Technology, Atlanta, Progress Report to Lockheed Georgia Co., Grant 08733, Oct. 1983.

[4] Kachanov, L.M., "Separation of Composite Materials," *Mekhanika Polimerov*, No. 5, 1976, pp. 918-922.

[5] Simitses, G.J., Sallam, S., and Yin, W.-L., "Effect of Delamination on Axially-Loaded Homogeneous Laminated Plates," *AIAA Journal*, Vol. 23, 1985, pp. 1437–1444.